

## THE INFLUENCE OF DRY SLIDING ON PRECIPITATION HARDENING BEHAVIORS OF Al-Cu-Si ALLOY

M. Zandrahimi and A. Rezvanifar

\* M.zandrahimi@mail.uk.ac.ir

Received: April 2011

Accepted: January 2012

Department of Materials Science and Engineering, ShahidBahonar University of Kerman, Kerman, Iran.

**Abstract:** Cold working performed before an aging treatment has a significant effect on size and amount of precipitate produced. This could be caused by the increase in defect density, such as vacancies and dislocations. In this research, the Al-Cu-Si alloy was solution-treated, wear-tested and then artificially aged for a period of 1–5 h. Changes in the amount of precipitate, in the lattice parameter of the matrix, and in the precipitates are measured by X-ray diffraction and then calculated. It was observed that performing a wear test before the aging treatment was done significantly increased the amount of precipitate, while wear rate decreased.

**Keywords:** Dry sliding, X-ray diffraction, lattice parameter, mass fraction

### 1. INTRODUCTION

The addition of Cu considerably increases the strength of Al-Si alloys due to the precipitation of a much dispersed Al<sub>2</sub>Cu phase during aging, which leads to a higher hardness [1, 2]. The degree of strengthening that is obtained depends on the volume fraction, shape and structure of the precipitates [1, 3, 4,5] and nature of the interface between the metastable phases and the Al matrix [4,6]. It is generally accepted that deformation is associated with the formation of a large amount of microstructural defects in solids, e.g., vacancies and dislocations [7]. Since these regions have a high free energy per atom, they will be the first to become unstable during transformation [8]. They act as short circuit paths for solute atoms [7,9]. Nucleation takes place preferably at these places, which are suitable for heterogeneous nucleation [2, 8, 10 and 11]. For Al alloys, it is also reported that intermediate plastic deformation increases the aging rate and improves the strength that is reached by conventional aging [12]. It is believed that very high strains lead to metastable phase extension and enhanced solid solubility [13].

Dutikiew and his co-workers [14] investigated the effect of plastic deformation on the properties of AA6000 alloys; they found that the precipitates mainly formed at the dislocations and that their density increased with increasing

deformation. However, the presence of dislocations generally results in an acceleration of the precipitation kinetics and coarsening of the precipitates [15,16]. Sliding contact between the surfaces of ductile materials is often accomplished with severe plastic deformation adjacent to the contact surface [17]. A large shear strain is induced in the subsurface region during the sliding wear process [18]. The ridges on both sides of an isolated wear track are plastically deformed regions that contain a high density of dislocations, which present a high internal energy [17]. Because of the small size of precipitates and high dislocations density which are generated as a consequence of severe plastic deformations and strain fields' related to precipitates, identifying them with TEM is very difficult [19]. In many cases, this leads to uncertainty. The crystal structure could be determined from the intensities and the angular position of the Bragg peaks in the diffraction pattern [4]; therefore, through investigation of changes in diffraction peaks, it is possible to obtain a great deal of information about the effects of precipitates in the structure.

In many tribological applications of aluminium alloys, the temperature of interface is high. This increases the solubility of the elements in the matrix during wear. The aim of this research is to investigate the changes which occur in the type, quantity and size of the precipitates in the region of wear.

## 2. EXPERIMENTAL PROCEDURE

### 2. 1. Samples Preparation

The Al-Si alloy had the following composition (wt%): Cu 6.52, Si 5, Mg 0.31 and Fe 0.27. The aluminium alloy was prepared by melting Al (99.7%purity) and Cu (99.5%purity) with Al-75%Si and Al-50%Mg master alloys; the master alloys were prepared by mechanical alloying. In this process, pure Al alloy was initially placed inside a graphite crucible and heated to 800°C in a resistance-heated furnace; then, the master alloy was added to the melt and stirred gently for 3 min. Copper, in the form of chips, was also added to the melt at a temperature of 800°C. The melts were held for 20 min for homogenisation and poured into a permanent metallic mould (180mm × 100mm × 10mm) at a temperature of 725°C. The mould was made of 10-mm-thick steel.

### 2. 2. Heat Treatment and Wear Investigation

To investigate the effect of wear on the precipitates, different heat treatments were designed to control both the precipitation behaviour and the aging, as shown in Fig. 1. The first procedure was a solution treatment at 490±5°C for 4 hr followed by cold water

quenching (<40 °C). Some specimens were held at room temperature for 2 h and were then aged at 180 °C for 1 hr (P<sub>1</sub>). Other specimens were wear tested at room temperature and aged at 180°C for 1 h (P<sub>2</sub>). All of the heat treatments were performed in an air-circulating furnace. The heat treatment process is outlined in Fig. 1.

The wear test was carried out with a pin-on disc instrument. The size of the test specimen was 70×70×6 mm<sup>3</sup>. Before the test, the surface of the samples was polished with a lath and cleaned in an ultrasonic bath that contained ethanol. Steel pins with a hardness of 59 RC were used as a counterface. The pin in the wear test has a 5-mm diameter and a 50-mm length. The wear tests were conducted at room temperature with a relative humidity of about 40 to 50%. A sliding speed of 0.21 m/s and a normal load of 220 N were applied. The total sliding distance was 1000 m. The aging treatment was carried out at a temperature of 180°C for a period of 1 to 5 hrs in the first and second path.

To investigate the effect of wear on the removal of material after the solution treatment, the worn samples were studied with a scanning electron microscope (SEM) (CAM SCAN 2300mv). The microhardness of the wear subsurface was measured by using a Vickers pyramidal indenter.

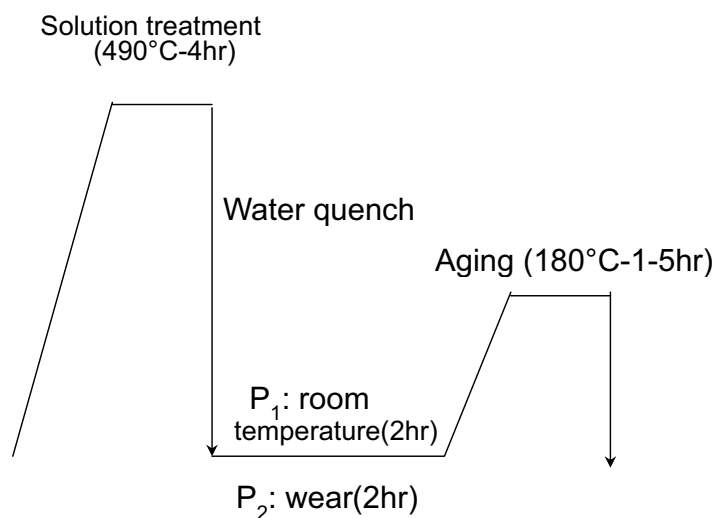


Fig. 1. Schematic diagram of heat treatment

### 2. 3. X-ray Diffraction Analysis

The X-ray diffraction (XRD) profile for each sample was recorded from the surface of the specimens before and after the wear test with a PHILIPS 1710 X-ray diffractometer that used Cu K $\alpha$  radiation. All of the diffraction profiles were obtained by varying the 2 $\theta$  from 35 to 142° with a step scan of 0.02. The amount of precipitates was determined by using a semi-quantitative analysis[20].

## 3. RESULTS AND DISCUSSION

### 3. 1. Effect of Wear on As-Cast Alloy

Figure 2 shows X-ray diffraction patterns of as-cast and worn samples of the Al-Cu-Si alloy that was wear-tested under an applied load of 126 N. After the wear test, a peak shift towards higher angles was observed (Fig. 2a). This indicates that the lattice parameter decreased, which was probably due to partial dissolution of the precipitates or compressive stresses generated owing to the wear [21]. The mass fraction of phases was calculated on the basis of a semi-

**Table 1.** Results of mass fraction of phases calculated on the basis of semi- quantitative analysis to X-ray diffraction before any heat treatment

| Specimen         | Mass fraction (%) |                    |      |
|------------------|-------------------|--------------------|------|
|                  | Al                | Al <sub>2</sub> Cu | Si   |
| Bulk sample      | 94.09             | 3.12               | 2.48 |
| After wear(126N) | 95.79             | 1.90               | 2.3  |

quantitative analysis, as shown in Table 1. After the wear test, the mass fraction of Al<sub>2</sub>Cu was reduced, but there was no significant change in the amount of Si (because dissolution of Si in an Al matrix is limited); therefore, with the second factor, copper dissolution was more effective in reducing the lattice parameter.

After wear, aluminium oxides and intermetallic compounds were not observed in the diffraction peaks. This result is in agreement with the findings of Chen et al. [22]. A comparison of the X-ray patterns from the as-cast and worn samples revealed that the peaks of the worn samples broadened (Fig. 2b). Peak broadening is due to grain refinement and lattice distortions in the

**Table 2.** Peak intensities measured on different planes before and after sliding

| Specimens        | Intensity |        |        |        |       |       |        |       |       |
|------------------|-----------|--------|--------|--------|-------|-------|--------|-------|-------|
|                  | (111)     | (200)  | (220)  | (311)  | (222) | (400) | (331)  | (420) | (422) |
| Bulk sample      | 918.14    | 394.55 | 321    | 474.65 | 61.72 | 68.40 | 160.71 | 176   | 72.15 |
| After wear(126N) | 563.35    | 172.36 | 122.06 | 180.36 | 99.96 | 99    | 73     | 70    | 74    |

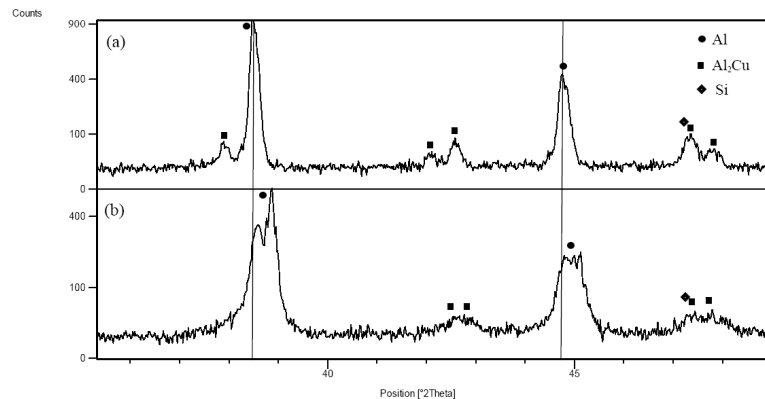


**Fig. 2.** The X-ray spectrum that were obtained from the a) bulk sample and b) after wear at a load of 126 N.

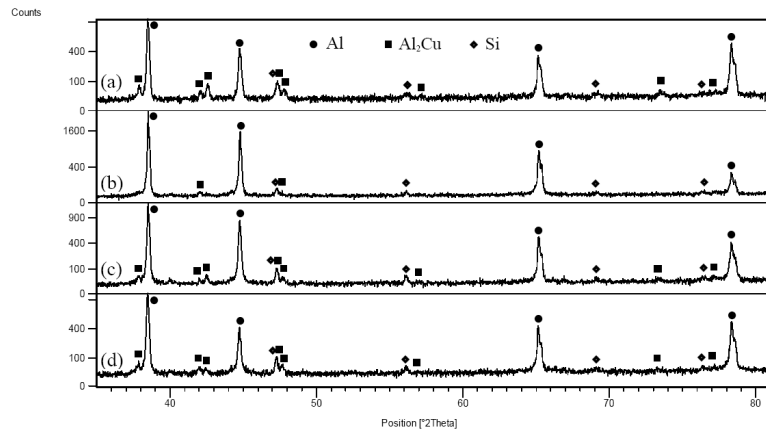


**Fig. 3.** A comparison between the X-ray diffraction patterns before and after the heat treatment (path 1) in the (a) as-cast sample, (b) 1 hr of aging, (c) 3 hrs of aging and (d) 5 hrs of aging

subsurface region [23].

Quantitative data on the intensities of the (111), (200), (220), (311), (222), (400), (331), (420), and (422) peaks are listed in Table 2. Peak intensities of the worn samples decreased compared with the intensity of the original sample. This is due to atomic rearrangement and enhancement of vacancies after cold working [24].

### 3. 2. Investigation of Heat Treatment

#### 3. 2. 1 Study of Path 1 (P1)

A comparison of X-ray diffraction patterns of the as-cast samples and the samples with different aging times, which underwent path 1 heat treatment, are shown in Figure. 3. As shown the percentage of precipitate increased with aging time (see Table 3 and Fig. 3).

**Table 3.** Results of mass fraction of phases calculated on the basis of semi- quantitative analysis to X-ray diffraction for path 1(P1)

| Aging time (hrs) | Mass fraction(%) |                    |      |
|------------------|------------------|--------------------|------|
|                  | Al               | Al <sub>2</sub> Cu | Si   |
| As-cast sample   | 94               | 3.12               | 2.48 |
| 1                | 97.87            | 0.67               | 1.51 |
| 3                | 95.61            | 1.62               | 2.67 |
| 5                | 95.81            | 2.19               | 1.98 |

The lattice parameters that were calculated for the Al phase as a function of Miller indices and for different aging periods are listed in Table 4. After aging, the lattice parameter changed significantly. Gue and Sha suggested that the change in the lattice parameter of the Al-Si-Cu alloy's matrix due to aging, which is measured from the X-ray diffraction

**Table 4.** Lattice parameters calculated for Al phase as a function of the miller indices of Bragg1(P1)

| Planes | Lattice parameter ( A°) |            |                  |         |         |                  |         |         |
|--------|-------------------------|------------|------------------|---------|---------|------------------|---------|---------|
|        | No heat treatment       |            | Path 1           |         |         | Path 2           |         |         |
|        | bulk                    | After wear | Aging time (hrs) |         |         | Aging time (hrs) |         |         |
|        |                         |            | 1                | 3       | 5       | 1                | 3       | 5       |
| (111)  | 4.04686                 | 4.02463    | 4.04393          | 4.04403 | 4.04716 | 4.04251          | 4.04372 | 4.04716 |
| (200)  | 4.04587                 | 4.02930    | 4.04270          | 4.04433 | 4.0469  | 4.04013          | 4.04296 | 4.04201 |
| (220)  | 4.04188                 | 4.03407    | 4.04227          | 4.04188 | 4.04503 | 4.03797          | 4.04227 | 4.04409 |
| (311)  | 4.04271                 | 4.03425    | 4.04254          | 4.04271 | 4.04245 | 4.04098          | 4.04349 | 4.04154 |
| (222)  | 4.04224                 | 4.03323    | 4.04188          | 4.04224 | 4.04196 | 4.04059          | 4.04357 | 4.04124 |

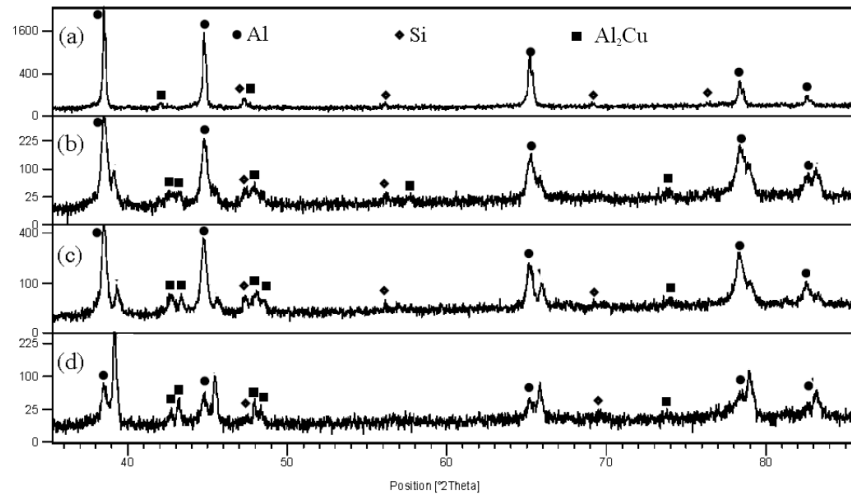


Fig. 4. A comparison between the X-ray diffraction patterns for path 1 and path 2: (a) path 1, 1 hr of aging; (b) path 2, 1 hr of aging, (c) path 2, 3 hrs of aging and (d) path 2, 5 hrs of aging

profile, is correlated to the fraction of the  $Al_2Cu$  phase that forms during aging [1].

Because of the solution treatment, a large amount of precipitate and particles are dissolved in the matrix, and after approximately 1 h of aging, the lattice parameter of aluminium is less than it was before heat treatment (Table 4). This is attributed to shrinkage of the lattice, which is due to the solution's alloying elements (Si or Cu) having smaller atomic radii than Al. Because solutes leave the matrix as aging time is increased, the magnitude of aluminium's lattice parameter is seen to progressively increase.

### 3. 3. Study of Path 2 (P2)

It is obvious from the data in Table 5 and from the diffraction peaks (Fig.4) that the amount of precipitate that formed in the second heat treatment process was greater than that formed in the first. During the wear test, severe plastic deformation took place; therefore, the dislocation density at the sliding contact area increased [25, 26]. These dislocations are favourable nucleation sites for precipitates and short-circuit diffusion paths for solutes [27]. As previously mentioned, the amount of  $Al_2Cu$  increased with aging time (Table 5). Furthermore, when the wear test was performed after the solution treatment, the supersaturated elements in the matrix increased;

therefore, a higher driving force for precipitate formation was generated.

Diffraction peak broadening decreased as aging time increased (Fig. 4). One effective factor in this case is the annihilation of dislocations, which is due to recovery and also nucleation of precipitates on dislocations [28].

A comparison of the Al matrix's lattice parameter for the samples that were aged for 1 h (Table 4) shows that there is a significant reduction in path 2 compared to path 1. There are two possible reasons for this:

1. Cold work deformation, which produces compressive stresses;
2. Enhancement of super saturation of the matrix (dissolving extra solute atoms), which provides a higher driving force for the formation of precipitates.

Table 5. Results of mass fraction of phases calculated on the basis of semi- quantitative analysis for path 2(P2) to X-ray diffraction

| Aging time (hrs) | Mass fraction (%) |          |      |
|------------------|-------------------|----------|------|
|                  | Al                | $Al_2Cu$ | Si   |
| 1                | 92.35             | 3.88     | 2.62 |
| 3                | 91.61             | 4.47     | 2.50 |
| 5                | 75.34             | 6.86     | 0.40 |

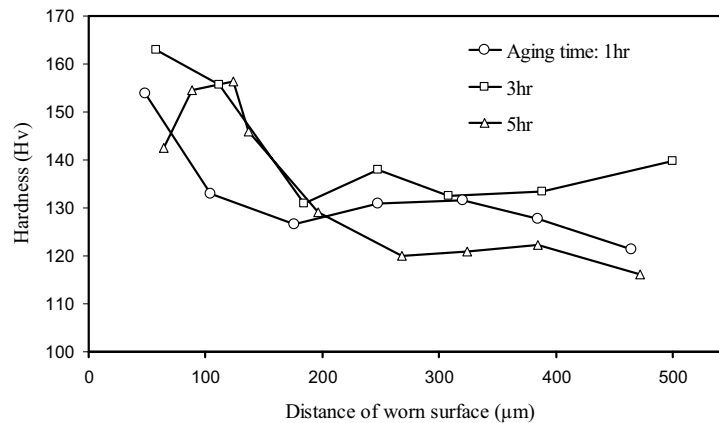


Fig. 5. Vickers microhardness as a function of the distance from the worn surface.

Figure 5 shows a plot of hardness of the heat-treated samples as a function of depth below the wear surface after testing. Hardness of the regions decreased as depth increased below the wear surface. The region closest to the wear surface experienced the maximum deformation, evident in the formation of the finest microstructural features and rise in precipitate density in that region.

Decrease in hardness was observed only up to a specific depth; hardness remained practically unchanged beyond this critical depth. Decrease in hardness of the subsurface area after artificial aging for 5 h is due to coarsening of the precipitates.

It is obvious that copper reduced the amount of adhesion during the wear tests on the Al-Si alloys in such a way that the particles scattered after detaching from the surface (Fig. 6) [29]. Therefore, the amount of plastic flow was significantly reduced. An investigation of the worn surface revealed that white layers were not present on it (Fig. 6); thus, it can be concluded that temperature did not increase considerably during the wear test.

Figure 7 shows the wear rate for the samples treated through path 2. As shown, specific wear rate decreased with sliding distance. It can be assumed that the formation of precipitates during sliding plays a more effective role in reducing wear rate than work hardening through cold work.

Variation in the lattice parameter of the  $\text{Al}_2\text{Cu}$

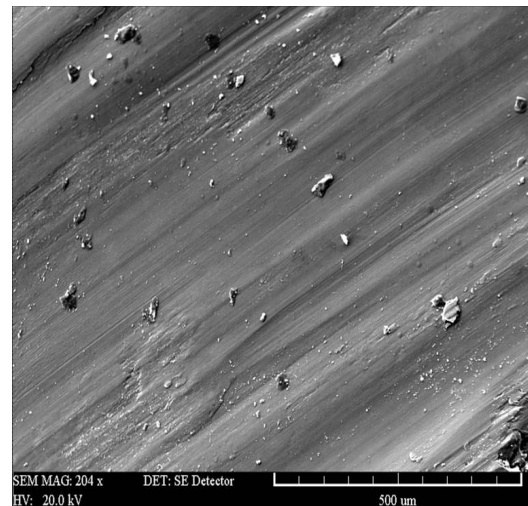


Fig. 6. Variations in the wear rate as a function of the sliding distance after the solution treatment.

as a function of the heat treatment and artificial aging is presented in Table 6. Due to interfacial strains, which are caused by the interaction of precipitate with the surrounding Al lattice, the shape and volume of the precipitate's unit cell may be different than that without the influence of the Al lattice [30]. It was found that lattice parameter size in  $\text{Al}_2\text{Cu}$  precipitate (a and c) increased after aging; however, in samples that were wear-tested, the magnitude of the lattice parameters decreased.

Most of the changes were generated in the c-axis of the precipitate, which resulted in better



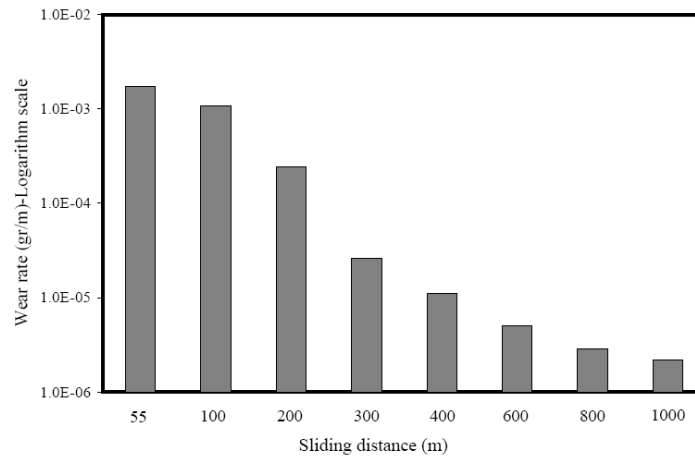


Fig. 7. Variations in the wear rate as a function of the sliding distance after the solution treatment

Table 6. Lattice parameters calculated for Al<sub>2</sub>Cu phase

| Specimens    | Lattice parameter ( Å ) |        |        |
|--------------|-------------------------|--------|--------|
|              | a                       | c      | c/a    |
| Base sample  | 0.6064                  | 0.4880 | 0.8047 |
| Path 1- 1hrs | 0.6068                  | 0.4888 | 0.8055 |
| Path 1- 3hrs | 0.6074                  | 0.4885 | 0.8042 |
| Path 1- 5hrs | 0.6076                  | 0.4896 | 0.8058 |
| Path 2- 1hrs | 0.5992                  | 0.4807 | 0.8022 |
| Path 2- 3hrs | 0.5976                  | 0.4791 | 0.8017 |
| Path 2- 5hrs | 0.5977                  | 0.4812 | 0.8052 |

coherency with the Al matrix. The Al matrix is aligned with the precipitates in certain directions. Therefore, the distance of all planes does not change similarly and some of the planes ((200), (111), and (220)) show more incrimination (Table 4). Strain fields that were generated around the precipitate prevented the movement of dislocations; therefore, after an aging period of 3 h, the hardness value increased [9] (Fig.5).

Gradual increase aging time to 5 h led to the precipitate interface being replaced with misfit dislocations, which caused relaxation of the matrix and the precipitate. Therefore, the value of the precipitate parameter began to increase, which in turn caused a decrease in hardness [31] (Fig. 5). It was found that the c/a ratio decreased considerably in the worn samples (Table 6); this was due to further alignment of the Al matrix

with the precipitate in certain directions as a consequence of larger precipitate density. Therefore, sphericity of the precipitates decreased, and the precipitate particles showed a preferred orientation. This was more evident in samples that were aged for 3 h, whereas, in samples that were aged for longer periods, the preferred orientation between precipitate and matrix was less apparent, due to the decrease in the fit between them.

#### 4. CONCLUSIONS

1. There is a significant decrease in the magnitude of the cast alloy's lattice parameter due to wear. This is a result of two factors: (1) compressive stresses due to wear and (2) dissolution of precipitate in the matrix. Because dissolution of Al<sub>2</sub>Cu is greater than that of Si, the extent to which Al<sub>2</sub>Cu causes a decrease the Al lattice parameter is greater than that does Si.
2. Performing the wear test after the solution treatment increases the supersaturated elements in the matrix; therefore, a higher driving force for precipitate formation was generated.
3. Because of the solution treatment, alloying elements dissolve in the matrix, which leads to a reduction in the lattice parameter. Because these elements (Cu and Si) have smaller atomic radii than Al, through aging and precipitate formation, lattice parameter

increases.

4. Wear increases the percentage of precipitates in solution-treated Al alloys. The formation of these precipitates increases the wear resistance.

## REFERENCES

1. Guo, Z., Sha, W., "Quantification of precipitate fraction in Al-Si-Cu alloys". *Mater. Sci and Eng A.*, 2005, 392, 449-452.
2. Waterloo, G., Hansen, V., Gjønnes, J., and Skjervold, S.R., "Effect of predeformation and preaging at room temperature in Al-Zn-Mg-(Cu,Zr) alloys". *Mater. Sci and Eng A.*, 2001, 303, 226-233.
3. Wang, G., Sun, Q., Feng, L., and Hui, L., "Effects of Cu, Mg contents and heat treatment on tensile, thermal stability and wear properties of Al-14.5Si-Cu-Mg alloys". *Mater and Design.*, 2007, 28, 1001-1005.
4. Novelo-Peralta, O., Gonzalez, G., and Lara-rodriguez, G.A., "Characterization of precipitation in Al-Mg-Cu alloys by X-ray diffraction peak broadening analysis". *Mater. Charac.*, 2007, 59, 773-780.
5. Shokuhfar, A., Ahmadi, S., Arabi, H. and Nouri, S., "Mechanics of precipitates in an Al-Cu-Li-Zr alloy using DSC technique and electrical resistance measurements". *Iranian Journal of Materials Science & Engineering.*, 2009, 6.(3) 15-20.
6. Anjabin, N., Karimi Taheri., "The effect of aging treatment on mechanical properties of AA6082 alloy: modeling experiment". *Iranian Journal of Materials Science & Engineering.*, 2010, 7 (2), 14-21.
7. Yassar, R., Field, D., and Weiland, H., "The effect of cold deformation on the kinetics of the  $\alpha'$  precipitates in an Al-Mg-Si alloy". *Metal. Mate. Transactions A.*, 2005, 36, 2059-2065.
8. Martin J., "Precipitation Hardening" 1rd Ed, 1968, pp. 8-104.
9. Porter, D. A., Easterling, K. E., "Phase transformations in metals and alloys" 2rd Ed, 1992.
10. Gubicza, J., Schiller, I., Chinh, N., Illy, j., Horita, Z. and Langdon, T. G., "Diffusion analysis across grain boundary in Al-3.7mass% Cu Alloy using analytical electron microscopy". *Mater. Sci. Eng A.*, 2007, 460-461, 77-85.
11. Tekmen, C., Cocen, U., J. *Mate. Sci. Lett.*, "Role of cold work and SiC volume fraction on accelerated age hardening behavior of Al-Si-Mg/SiC composites". *Mate. Sci. Lett.*, 2003, 22, 1247-1249.
12. Sun, Y., Baydogan, M. and Cimenoglu, H., "The effect of deformation on the wear resistance of an aluminium alloy". *Mater. Lett.*, 1999, 38, 221-226.
13. Gao, Z. G., Zhang, X. and Chen, M., "Influence of strain rate on the precipitate microstructure in impacted aluminum alloy". *Scr. Mater.*, 2008, 59, 983-986.
14. Dutkiewicz, J., Litynska, L., "The effect of plastic deformation on structure and properties of chosen 6000 series aluminium alloys". *Mater. Sci. Eng A.*, 2002, 324, 239-243.
15. Birol, Y., "Pre-straining to improve the bake hardening response of a twin-roll cast Al-Mg-Si alloy". *Scripta. Materialia.*, 2005, 52, 169-173.
16. Akhlaghi, F., Zahedi, H., Sharifi, M., "Effect of reinforcement volume fraction, reinforcement size and solution heat treatment on the microstructure of the two differently processed A35 & SICP composites". *Iranian Journal of Materials Science & Engineering.*, 2004, 1 (2), 9-15.
17. Bateni, M., Szpunar, J., Wang, W. and Li, D. Y., "Wear and corrosion wear of medium carbon steel and 304 stainless steel". *Wear.*, 2006, 260, 116-122.
18. Tjong, S., Wu, S. and Liao, H., "Wear behaviour of an Al-12% Si alloy reinforced with a low volume fraction of SiC particles". *Compos. Sci. Technol.*, 1998, 57, 1551-1558.
19. Roven, H., Liu, M. and Werenskiold, G., "Dynamic precipitation during severe plastic deformation of an Al-Mg-Si aluminium alloy". *Mater. Sci. Eng A.*, 2008, 483-484, 54-58.
20. Moore, D., Reynolds, R., *X-ray Diffraction and the Identification and Analysis of Clay Minerals*, 1989, New York, pp. 448.
21. Korchef, A., Championb, Y. and Njah, N., "X-ray diffraction analysis of aluminium containing  $Al_8Fe_2Si$  processed by equal channel



- angular pressing”, *J. Alloy Compd.*, 2007,427,176-182.
22. Chen, C., Yang, C. and Chao, C., “A novel method for net-shape forming of hypereutectic Al-Si alloys by thixocasting with powder preforms”.*Mater. Sci. Eng A.*,2005, 397,178-189.
  23. Gubicza, J., Balogh, L., Hellmig, R., Estrin, Y. And Ungar, T.,”Dislocation structure and crystallite size in severely deformed copper by X-ray peak profile analysis”.*Mater. Sci. Eng A.*, 2005,400-401, 334-338.
  24. Guinebretiere, R., “X-ray Diffraction by Polycrystalline Materials”, 1rd Ed, 2007, pp.197-233.
  25. Stachowiak, W., Batchelor, A., *Engineering Tribology*, 3rd Ed, 2005, pp. 560-650.
  26. Rezvanifar, A., Zandrahimi, M.,”Evaluation of dislocation structure and crystallite size in worn Al-Si alloy by X-ray diffraction”.*Iranian Journal of Materials Science & Engineering.*, 2010, 7(1), 32-38.
  27. Weiland, A., Hultman, L., Wahlstorm, U. and Presson, C.,”Internal stress and microstructure of SiC reinforced aluminium alloy 2014”. *Acta. Mater.*, 1998, 46, 5271-5281.
  28. Fatay, D., Bastarash, E., Nyilas, K., Dobatkin, S.,Gubicza, J. and Ungar, T., “X-ray diffraction study on the microstructure of an Al-Mg-Sc-Zr alloy deformed by high pressure torsion”. *Metallkd.*,2003, 94, 842-847.
  29. Aminul Islam, Md., Haseeb, A. S. M. A.,”A comparative wear study on heat-treated aluminium–lithium alloy and pure aluminium”. *Mater. Sci. Eng A.*, 1999, 268,104-108.
  30. Van Huis, M., Chen, J., Sluiter, M. and H. W. Zandbergen.,”Phase stability and structural features of matrix-embedded hardening precipitates in Al-Mg-Si alloys in the early stages of evolution”.*Acta.Mater.*, 2007, 55, 2183-2199.
  31. Mukherji, D., Gilles, R., Barbier, B. and Genovese, D., “Lattice misfit measurement in Inconel 706 containing coherent  $\gamma$  and  $\gamma'$  precipitates“. *Scr. Mater.*, 2003,48, 333-339.